Eur Biophys J (1997) 26: 447–459

ARTICLE

Patrick Garidel · Christof Johann · Lutz Mennicke
Alfred Blume

The mixing behavior of pseudobinary phosphatidylcholine-phosphatidylglycerol mixtures as a function of pH and chain length

Received: 17 March 1997 / Accepted: 4 July 1997

Abstract The miscibility of phosphatidylcholine (PC) and phosphatidylglycerol (PG) with different chain lengths (n = 14, 16) was examined by differential scanning calorimetry (DSC) at pH 2 and pH 7. The determination of the coexistence curves of the phase diagrams was performed using a new procedure, namely the direct simulation of the heat capacity curves as described recently (Johann et al. 1996, Garidel et al. 1997). From the simulations of the heat capacity curves first estimates for the nonideality parameters for nonideal mixing as a function of composition were obtained and phase diagrams were constructed using temperatures for the onset and offset of melting which were corrected for the broadening effect caused by a decrease in cooperativity of the transition. In most cases, the composition dependence of the nonideality parameters indicated nonsymmetric mixing behavior. The phase diagrams were further refined by simulations of the coexisting curves using a four-parameter model to account for nonideal and nonsymmetric mixing in the gel as well as in the liquid-crystalline phase. The mixing behavior of the systems was analyzed as a function of pH and chain length difference to elucidate the effect of these two parameters on the shape of the phase diagrams. At pH 7 the phase boundaries are much closer together and a narrower coexistence range is obtained compared to the corresponding phase diagrams at pH 2. For DPPC/DMPG at pH 2, the shape of the phase diagram and the strongly positive nonideality parameter ρ_1 for the liquid-crystalline phase indicates an upper azeotropic point. This indicates an unusual behavior of the system, namely more pronounced clustering of like molecules in the liquid-crystalline phase compared to the gel phase.

P. Garidel · L. Mennicke
Fachbereich Chemie, Universität Kaiserslautern,
D-67653 Kaiserslautern, Germany

C. Johann · A. Blume (✉)
Institut für Physikalische Chemie, Fachbereich Chemie,
Martin-Luther-Universität Halle-Wittenberg,
D-06108 Halle, Germany,
(e-mail: blume@chemie.uni-halle.de)

Key words Phosphatidylcholine · Phosphatidylglycerol · DSC · Phase diagrams · Miscibility · Nonideality parameter

Introduction

Several reasons make it worthwhile to study pseudobinary mixtures of phosphatidylcholine (PC) with phosphatidylglycerol (PG) (Wiedmann et al. 1993). Phosphatidylglycerol is one of the major phospholipids in the membranes of plant leaves, algae, and many bacterial species (MacFarlane 1964). It is also present in small amounts in mammalian membranes. The major two classes of phospholipids within the lung surfactant are these two components (van Golde 1988; Goerke 1974; Clements 1977). For medical applications, saturated PCs are important in forming a condensed surface film resistant to collapse and the PG component (unsaturated or sometimes saturated hydrocarbon chains) is involved in the rapid movement to and away from the interface during the breathing cycle ("fluidizing-effect") (Bangham et al. 1979). It was also found that these two lipid classes are required for the formation of the lipid-protein aggregates, such as tubular myelin, located in the subphase of the lung alveoli (Cronan and Gelman 1975; Benson et al. 1984; Suzuki et al. 1989). Considering the interaction with apoliproteins in determining the surface activity of the surfactant, the lipid phase behavior has been suggested to be an important factor.

Vesicle preparations composed of synthetic PC/PG mixtures have been used to study the Ca^{2+}-mediated binding of γ-carboxy-glutamate-containing human prothrombin to negatively charged membrane surfaces (Dombrose et al. 1979; Tocanne et al. 1994). This is one of the several protein/lipid interactions that are thought to be crucial to the ability of PC/PG-mixtures to enhance in vitro by several thousand fold the rate of blood coagulation (Jackson et al. 1974; Barton and Findlay 1978).

Barton and Findlay (1978) have reported for the reaction prothrombin to thrombin (blood coagulant) that a

higher coagulation activity was observed with liquid-crystalline phase systems (e. g. PC/PG-mixtures), compared to mixtures in the gel state and that optimal activity occurred from a biphasic lipid system (lateral lipid-lipid phase separation e. g. DLPC-DMPG-Ca^{2+} system) (Verkleij et al. 1974). The authors mentioned: "a lateral lipid phase separation (fluid-solid or fluid-fluid) provides separate domains for binding of Ca^{2+}-dependent and Ca^{2+}-independent protein, their subsequent interactions proceeding in proximity to a transition zone (mismatch region) between the domains." The formation of domains in the liquid-crystalline phase, caused by low miscibility of the two components in the phase, is an interesting phenomenon which has recently attained much attention (Shimshick and McConnell 1973; Stier and Sackmann 1973; Lee et al. 1974; van Dijck et al. 1977; Hoekstra 1982 a, b; Metcalf et al. 1986; Glaser 1993; Almeida et al. 1993; Vaz 1994, 1995; Almeida and Vaz 1995).

In the late seventies, several studies focused their attention on the phase behavior of pure synthetic phosphatidylglycerols and mixtures (van Dijck et al. 1975, 1978; Jacobson and Papahadjopoulos 1975; Ranck et al. 1977; Watts et al. 1978; Findlay and Barton 1978; Wohlgemuth et al. 1980; Cevc et al. 1980; Harlos and Eibl 1980; Lentz et al. 1982). Recently, new studies on PC/PG-mixtures have been reported, particularly because in these mixtures the binding of multivalent cations can lead to domain formation in the liquid-crystalline phase (Lau et al. 1981; Borle and Seelig 1985; Macdonald and Seelig 1987; Wiedmann et al. 1993; Seelig et al. 1995).

In this paper we deal with the mixing behavior of synthetic phosphatidylcholines (PC) and phosphatidylglycerols (PG) with acyl chain lengths of n = 14, 16 at two different pH-values, namely pH 2 and pH 7. The following pseudobinary mixtures were analyzed by DSC: DMPC/DMPG, DPPC/DPPG, DMPC/DPPG and DPPC/DMPG.

The aim of this study is the determination of the pseudobinary phase diagrams as a function of pH. At pH 2 the PG headgroup is mostly protonated, whereas at pH 7 it carries a negative charge. Therefore, the headgroup interactions are modulated by a pH change. We apply a recently developed simulation procedure for the experimentally determined DSC curves (cp-curves) to obtain phase diagrams which are then further analyzed (Johann et al. 1996; Garidel et al. 1997).

Materials and methods

The synthetic lipids 1,2-dimyristoyl-*sn*-glycero-3-phosphorylcholine (DMPC), 1,2-dipalmitoyl-*sn*-glycero-3-phosphorylcholine (DPPC), 1,2-dimyristoyl-*sn*-glycero-3-phosphorylglycerol (DMPG, Na-salt), and 1,2-dipalmitoyl-*sn*-glycero-3-phosphorylglycerol (DPPG, Na-salt) were gifts from Nattermann Phospholipid GmbH (Cologne, Germany). The purity of the lipids was checked by thin-layer chromatography (TLC). After detection with a phosphorus sensitive spray and after charring with concentrated sulfuric acid (Hahn and Luckhaus 1956), only one spot was detected on the TLC-plate. Therefore, the lipids were used without further purification.

Lipid stock solutions in $CHCl_3 : CH_3OH$ (2 : 1, v : v) were prepared and mixed to obtain homogeneous mixtures at different molar ratios. The solvent was rapidly removed under an argon stream by carefully heating the samples. The lipid films were then held for 24 h in high vacuum to remove residual solvent traces. An appropriate amount of 0.1 M NaCl (in ultrapure water) was added to the dry lipid films and the samples were then vigorously vortexed for 5 min at 75 – 80 °C and additionally for 5 min at room temperature to get a homogeneous disperson. The pH of the samples was checked and corrected by an appropriate amount of HCl or NaOH. The measurements were done at pH 7 and pH 2. The total-lipid concentration was 2.5 mg/ml. The pH was measured before and after the DSC-experiment. No changes of the pH were observed.

Differential scanning calorimetry (DSC) measurements were performed with a MicroCal MC-2 scanning calorimeter (MicroCal, Inc., Northhampton, MA, USA). The heating rate was 1 °C/min. The shape of the thermograms was independent of heating rates as long as they were 1 °C/min or lower. Heating curves were measured in the temperature interval from 5 to 70 °C. The reproducibility of the DSC experiments was checked by comparing three heating scans of each sample at pH 7. Before and after the measurements the samples were checked by thin layer chromatography (TLC) and no degradation of the lipids was detected. At pH 2, only the first scan was used for the analysis because of increasing chemical degradation as detected by TLC after the second DSC scan.

Three independently prepared samples were measured to test the reproducibility of the sample preparation. The reproducibility of the DSC-experiments was ±0.1 °C for the main phase transition temperature T_m and ±0.2 kcal/mol for the main phase transition enthalpy ΔH_m.

Simulations

Calculation of the heat capacity curves

The calculation of heat capacity curves is based on the convolution of a heat capacity curve which describes a hypothetical phase transition with infinitely high cooperativity (cp^{id}) with a function that describes the broadening of the phase transition due to limited cooperativity (Mennicke 1995). The details of the method have been described elsewhere (Johann et al. 1996; Garidel et al. 1997).

The program requires as input the experimental heat capacity curve, the thermodynamic parameters of the pure lipid components (main phase transition enthalpies and transition temperatures) and the composition of the mixture. As variable parameters, the nonideality parameter ρ and the van't Hoff enthalpy ΔH_{vH} are introduced. As output we obtain the simulated heat capacity curve (cp^{sim}), the

Table 1 Thermodynamic data for the main phase transition of phospholipids in 0.1 M NaCl and in pure H_2O (denoted with the asterisks *). T_m = maximum of the cp-curve, $T_{1/2}$ = half-width of the transition, ΔH_c = calorimetrically determined transition enthalpy

Lipid	pH = 2			pH = 7		
	T_m /°C	$T_{1/2}$ /°C	ΔH_c /kcal · mol^{-1}	T_m /°C	$T_{1/2}$ /°C	ΔH_c /kcal · mol^{-1}
DMPC	26.0	0.9	6.45	24.0	0.5	7.36
DMPG	41.4	2.0	6.74	23.3	0.7	7.35
DPPC	41.6	0.8	8.37	41.4	0.8	9.15
DPPG	58.3	3.5	9.22	40.0	0.9	8.15
DMPC *	24.5	0.8	5.57	24.0	0.5	7.35
DPPC *	41.7	0.9	7.92	41.6	0.5	8.45

Table 2 Thermodynamic data for the pretransition of phospholipids in 0.1 M NaCl and in pure H_2O (denoted with the asterisks *): T_p = maximum of the cp-curve, $T_{1/2}$ = half-width of the transition, ΔH_c = calorimetrically determined transition enthalpy

Lipid	pH = 2			pH = 7		
	T_p /°C	$T_{1/2}$ /°C	ΔH_c /kcal · mol^{-1}	T_p /°C	$T_{1/2}$ /°C	ΔH_c /kcal · mol^{-1}
DMPC	18.7	2.7	0.54	15.5	1.5	1.56
DMPG	–	–	–	12.7	2.1	0.51
DPPC	35.9	2.3	0.96	34.5	2.9	1.39
DPPG	–	–	–	31.3	2.6	0.46
DMPC *	15.5	1.9	1.2	15.3	1.5	1.32
DPPC *	36.1	1.9	1.3	34.5	2.3	1.61

corresponding nonideality parameters ρ (ρ_g for the gel phase and ρ_1 for the liquid-crystalline phase) and the temperatures T(–) that describe the beginning and T(+) the end of the phase transition, respectively. These temperature data are then used for the construction and simulation of the complete phase diagrams. From the van't Hoff enthalpy the cooperative unit size c. u., defined as the ratio of the van't Hoff enthalpy and the calorimetrically measured main phase transition enthalpy, can be calculated.

Simulation of the phase diagrams

The phase diagrams were simulated with a model based on regular solution theory (Lee 1975 a, b; 1977 a, b; 1978; Tenchov 1985; Brumbaugh and Huang 1992). Because the simulation of the cp-curves indicated composition dependent nonideality parameters, a four-parameter approximation is used for nonsymmetric, nonideal mixing. For this model the excess free enthalpy (Gibbs free energy) of mixing, ΔG^E, is given as:

$$\Delta G^E = x(1-x)[\rho_1 + \rho_2(2x - 1)] \quad (1)$$

with x being the mole fraction of the second component. Therefore, two nonideality parameters ρ_1 and ρ_2 are obtained for both phases, the first one describing the nonideality at x = 0.5, the second one the dissymmetry (Mennicke 1995; Johann et al. 1996; Garidel et al. 1997).

Monte Carlo simulation of lipid lateral distribution

Monte Carlo simulations for lateral lipid distributions in the liquid-crystalline phase were carried out on a 80×80 two-dimensional triangular lattice with standard periodic boundary conditions using fixed mole fractions x and nonideality parameters determined from the simulations of the phase diagrams. To bring the system into equilibrium the Kawasaki method was used (Kawasaki 1972; Jan et al. 1984; Garidel et al. 1997). For the simulations of distributions at pH 7 the pure phases of the two components were used as a start configuration. Equilibrium was reached after $6 \cdot 10^7$ Monte Carlo steps. For simulations at pH 2 a random configuration of the two components as start configuration was used. In this case it was necessary to use $9 \cdot 10^8$ Monte Carlo steps to reach equilibrium.

Results

Pure components

All DSC experiments were performed in 0.1 M aqueous NaCl solution to ensure reproducible behavior by a sufficient ionic strength (Eklund et al. 1989). The pH dependence of the main phase transition of the phospholipids is summarized in Table 1, the corresponding results for the pretransition in Table 2.

At pH 2, the headgroup charge of PG is lowered by protonation of the phosphate group. This increases the transition temperature by approximately 18 °C. Watts et al. (1978) have determined the pK_{app} of PG to be 2.9 at physiological ionic strength whereas the intrinsic pK is probably much lower and around 1 (Boggs 1987; Tocanne and Teissié 1990). We conclude that under our conditions PG is mostly in its protonated state. Our results are in agreement with previous observations (Jacobson and Papahadjopoulos 1975; Träuble 1976; Träuble et al. 1976; Watts et al. 1978).

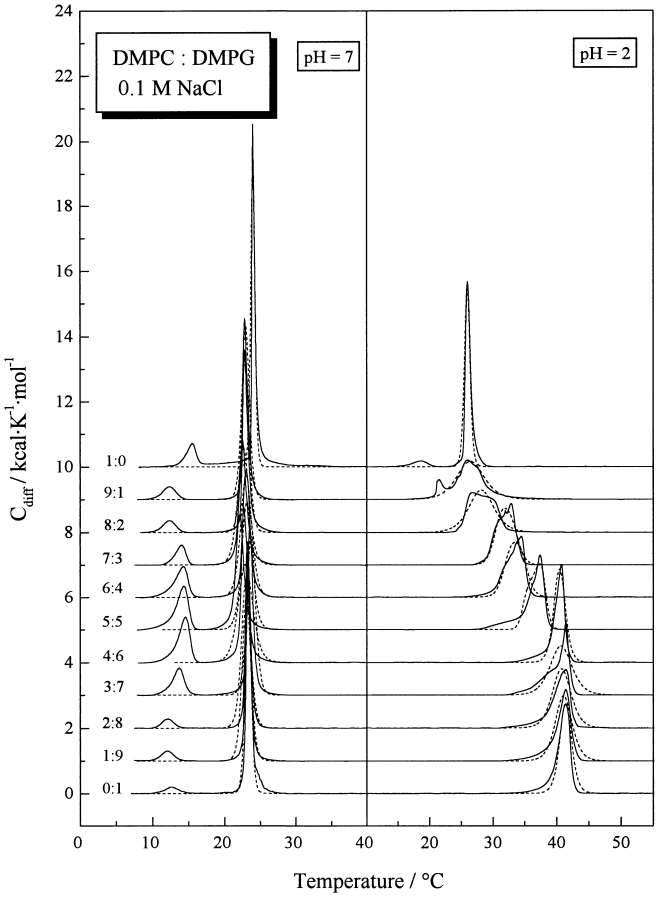

Fig. 1 DSC heating thermograms for the system DMPC/DMPG at various mole-ratios at pH 7 and pH 2: experimental cp-curve (*solid line*) and simulated cp-curve (*dotted line*)

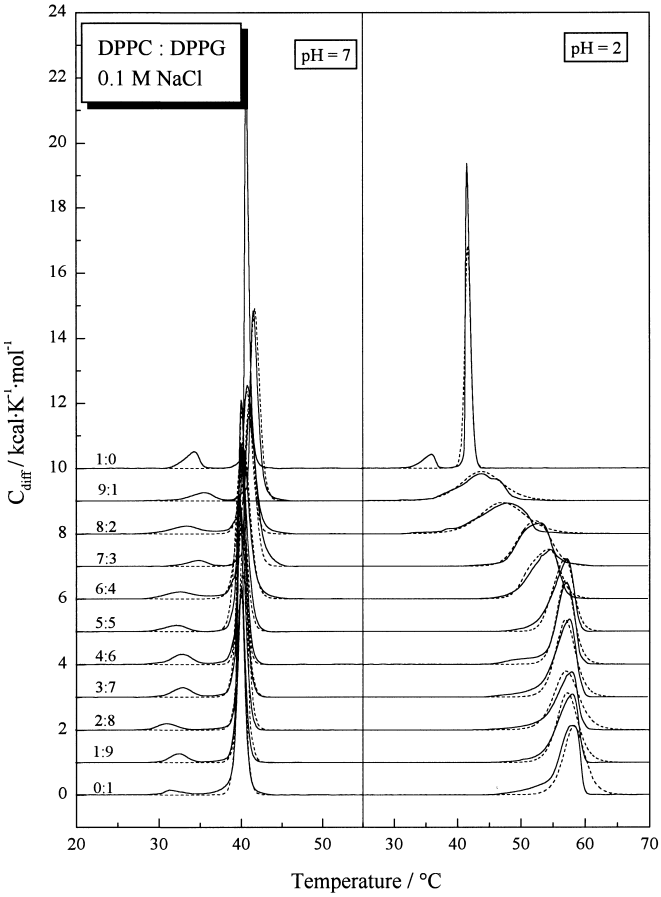

Fig. 2 DSC heating thermograms for the system DPPC/DPPG at various mole-ratios at pH 7 and pH 2: experimental cp-curve (*solid line*) and simulated cp-curve (*dotted line*)

At pH 7 PCs are zwitterionic lipids. At pH 2, only a small amount of PC ($pK_{app} < 2$) is probably protonated. If protonation of the phosphate group occurs, a hydrogen bond network can form, but on the other hand electrostatic repulsion between the positively charged $N^+(CH_3)_3$ groups increases. The former effect increases T_m, whereas electrostatic repulsion lowers T_m. This antagonistic effect results in only small changes of the phase transition temperature (Boggs 1987; Tocanne and Teissié 1990). From the small T_m change we conclude that PC is mainly zwitterionic under our conditions. Also, changes in ionic strength have only small effects on the thermotropic phase behavior of PCs (see Table 1). The small T_m increase seen for DMPC at pH 2 for the first DSC scan was observed before by Träuble and Eibl (1974). With decreasing pH, the transition enthalpies of the pure components and also of the mixtures decrease (see Table 1) with the exception of pure DPPG.

The pH-effects on the pretransition parameters can be summarized as follows (see Table 2): For PGs no pretransition is observed at pH 2 in accordance with previous reports (Sacré et al. 1979). The temperatures of the pretransition of the PCs are raised by 1.4 °C for DPPC and by 3.2 °C for DMPC and the transition enthalpies are slightly reduced.

Pseudobinary lipid mixtures

In Figs. 1–4, the DSC thermograms obtained at pH 2 and 7 for the four pseudobinary lipid systems are shown. The solid lines represent the experimentally measured cp-curves and the dotted lines are the simulated heat capacity curves cp^{sim} for the main phase transition. The measurements were performed in the temperature range from 5 to 70 °C, but only the temperature range in which phase transitions are observed is shown. In all cases, the simulation of the DSC-curves of the PC/PG-mixtures gives satisfactory fits.

From these fits we obtained the temperatures T(–) and T(+) (triangles in Figs. 5–8) which were used to construct the phase diagrams shown in Figs. 5–8. Based on these temperature data, the phase boundaries were fitted by a non-linear least squares fit using the four-parameter model described above (Johann et al. 1996; Garidel et al. 1997). This fitting procedure yields the nonideality parameters ρ

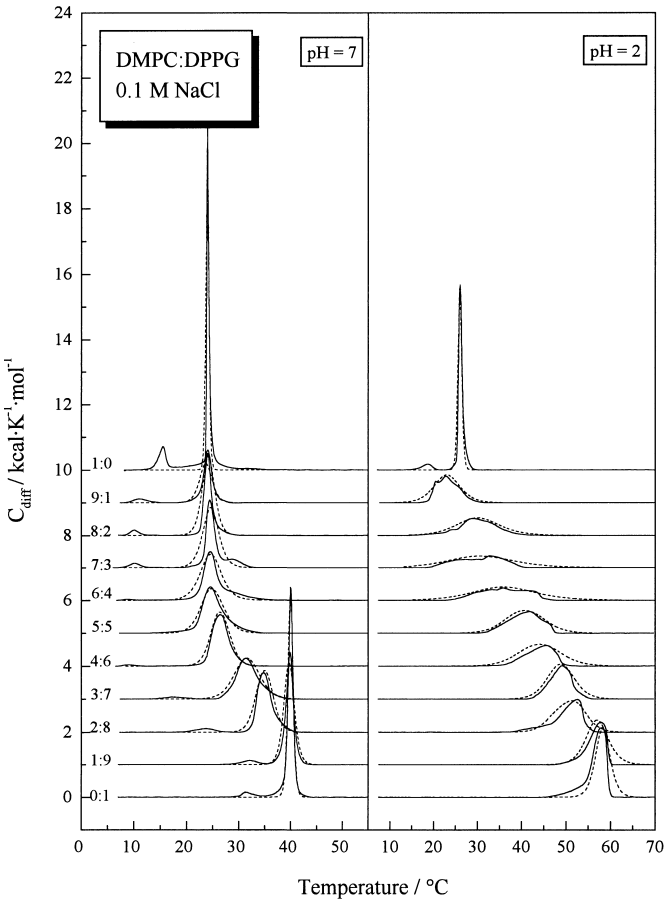

Fig. 3 DSC heating thermograms for the system DMPC/DPPG at various mole-ratios at pH 7 and pH 2: experimental cp-curve (*solid line*) and simulated cp-curve (*dotted line*)

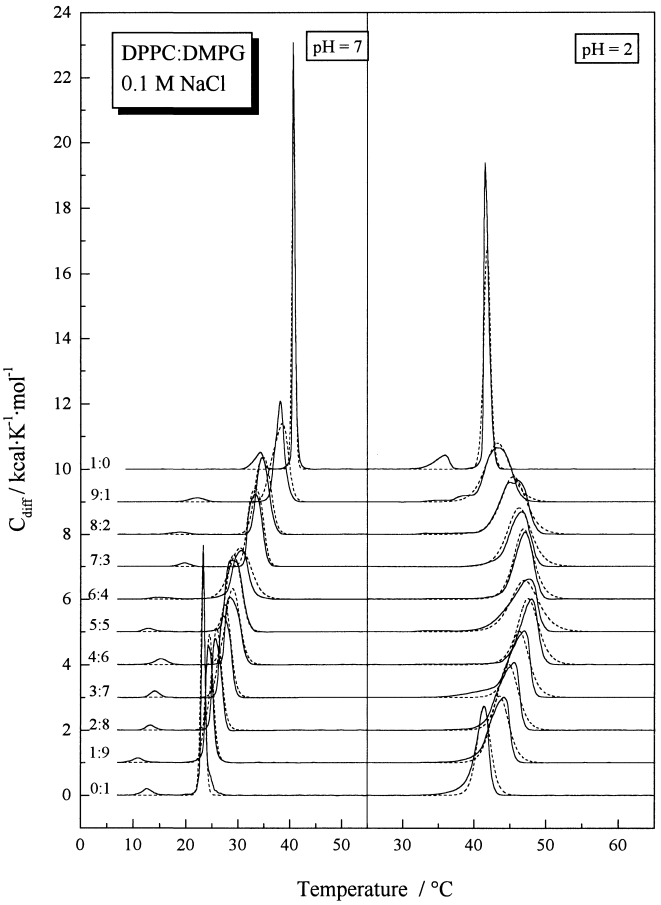

Fig. 4 DSC heating thermograms for the system DPPC/DMPG at various mole-ratios at pH 7 and pH 2: experimental cp-curve (*solid line*) and simulated cp-curve (*dotted line*)

for the liquid-crystalline and gel phase. The differences in the nonideality parameters between liquid-crystalline and gel state are $\Delta\rho_1 = \rho_{11} - \rho_{g1}$ and $\Delta\rho_2 = \rho_{12} - \rho_{g2}$ (index 1 for the liquid-crystalline phase and index g for the gel phase). The latter values are more precise than the absolute values for ρ (Johann et al. 1996). The temperatures T^{exp}(–) and T^{exp}(+) (circles in Figs. 5–8) obtained by the usual half-empirical procedure from the deviation of the experimental DSC curves from the baseline, corrected for the width of transition of the pure components weighted by their mole fraction (Mabrey and Sturtevant 1976), are also shown.

Figure 9 shows the phase transition enthalpies of the four systems at pH 7 as a function of composition. Figure 10 shows the $\Delta\rho$ ($\Delta\rho = \rho_1 - \rho_g$) values obtained from the direct simulation of the heat capacity curves using the two-parameter model described above and the corresponding values calculated from the nonideality parameters shown in Figs. 5–8. Figure 11 shows the cooperative unit size c.u. for the PC/PG mixtures as a function of composition at pH 2 and pH 7.

DMPC/DMPG

pH 7. With increasing amounts of either PG or PC first a slight decrease of the pretransition temperature to the $P_{\beta'}$ phase is observed before it increases again and reaches a maximum at $x_{DMPG} = 0.5$. The enthalpy of the pretransition ΔH_p shows a maximum at $x_{DMPG} = 0.5$ with ΔH_p = 3 kcal/mol whereas for the pure components the ΔH_p values are between 0.5 to 1.5 kcal/mol (see Table 2). The main phase transition temperature T_m is only a slightly lowered for equimolar mixtures. The transition enthalpies ΔH_m (ca. 6 kcal/mol) are nearly independent of composition.

The phase diagram at pH 7 (DMPG is singly charged) shows a very narrow coexistence range (see Fig. 5). The $\Delta\rho$ values obtained by the direct simulation of the cp-curves (Fig. 10) are in good agreement with the calculated parameters (c) using the relation $\Delta\rho_c = \Delta\rho_1 + \Delta\rho_2 \cdot (2x\text{-}1)$ (x: second component of the mixture) and the values shown in Fig. 5. The mixing behavior is very close to completely ideal. The negative ρ-values for the liquid-crystalline as well as for the gel phase indicate that compound formation is slightly more favorable than demixing.

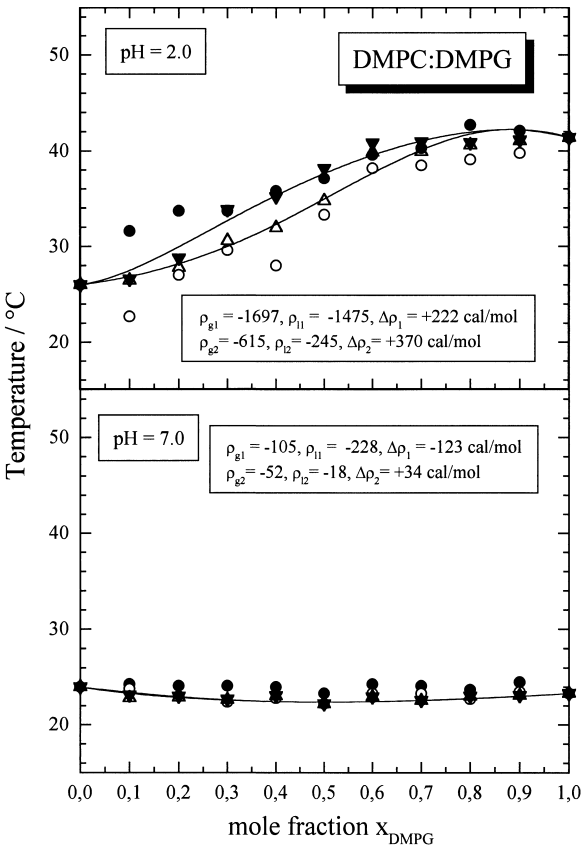

Fig. 5 Pseudobinary phase diagrams for the system DMPC/DMPG at pH 2 and pH 7 constructed from the simulated cp-curves. *Triangles* are T(–) and T(+) values obtained from the simulation of the cp-curves, *circles* are T^{exp}(–) and T^{exp}(+) values obtained by the usual empirical procedure. The *solid lines* are the coexistence lines calculated using the four-parameter model described in the text with the nonideality parameters shown in the *boxes*

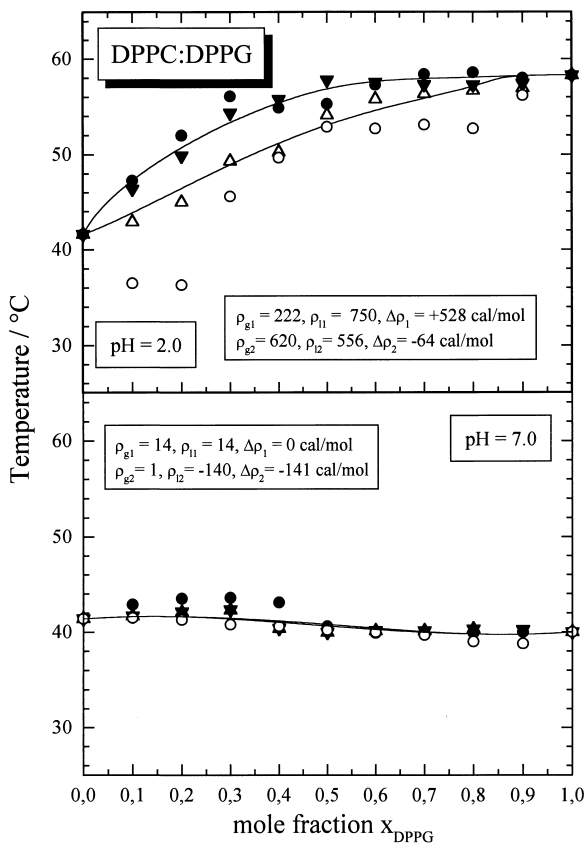

Fig. 6 Pseudobinary phase diagrams for the system DPPC/DPPG at pH 2 and pH 7 constructed from the simulated cp-curves. *Triangles* are T(–) and T(+) values obtained from the simulation of the cp-curves, *circles* are T^{exp}(–) and T^{exp}(+) values obtained by the usual empirical procedure. The *solid lines* are the coexistence lines calculated using the four-parameter model described in the text with the nonideality parameters shown in the *boxes*

pH 2. At pH 2 DMPG is protonated (Watts et al. 1978; Tuchtenhagen 1994). Protonation of DMPG shifts T_m up to nearly 40 °C due to the reduction in electrostatic repulsion and the increase in capacity for hydrogen bond formation between headgroups. No pretransition is observed for pure DMPG and for mixtures with DMPC.

The phase diagram has an S-shaped form, indicating highly asymmetric mixing behavior. The values of the nonideality parameters are negative for both phases, indicating complex formation between unlike molecules. The asymmetry is such, that for mixtures with large amounts of DMPG ($x_{DMPG} > 0.5$) the nonideality parameters are more negative than for mixtures with excess DMPC. This means that small amounts of protonated DMPG form complexes with DMPC more readily than vice versa.

DPPC/DPPG

pH 7. At pH 7, again a very narrow coexistence range is obtained. The mixing behavior is nearly ideal in both phases.

The ΔH_m-values are in the range of 9 kcal/mol and the transition enthalpies for the pretransition are in the range of 1 kcal/mol and, in contrast to the system DMPC/DMPG, independent of the composition of the mixtures.

pH 2. The thermograms for DPPC/DPPG are significantly different compared to the shorter chain analogues DMPC/DMPG. The DSC curves at pH 2 are broader (see Figs. 1 and 2) and the simulation of the phase diagram yields positive ρ values for both phases indicating demixing rather than complex formation. Test calculations with negative ρ values but the same $\Delta\rho_1$ and $\Delta\rho_2$-values gave phase diagrams with considerably narrower coexistence ranges (data not shown). The solidus curve shows an almost linear increase up to a mole fraction of $x_{DPPG} = 0.6$. At $x_{DPPG} = 0.9$ the solidus line touches the liquidus line and the coexistence range becomes very narrow. This shape of the phase diagram indicates an upper azeotropic point at $x_{DPPG} = 0.9$.

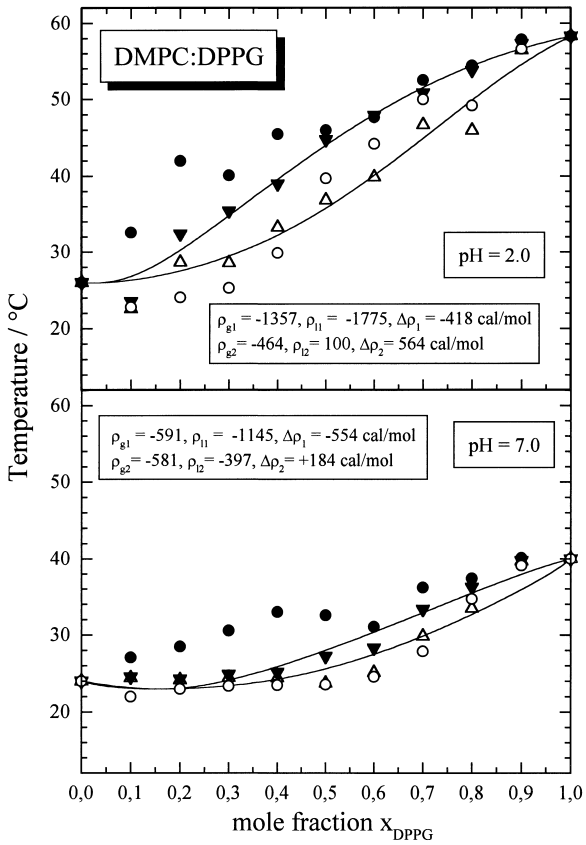

Fig. 7 Pseudobinary phase diagrams for the system DMPC/DPPG at pH 7 and pH 7 constructed from the simulated cp-curves. *Triangles* are T(–) and T(+) values obtained from the simulation of the cp-curve, *circles* are T^{exp}(–) and T^{exp}(+) values obtained by the usual empirical procedure. The *solid lines* are the coexistence lines calculated using the four-parameter model described in the text with the nonideality parameters shown in the *boxes*

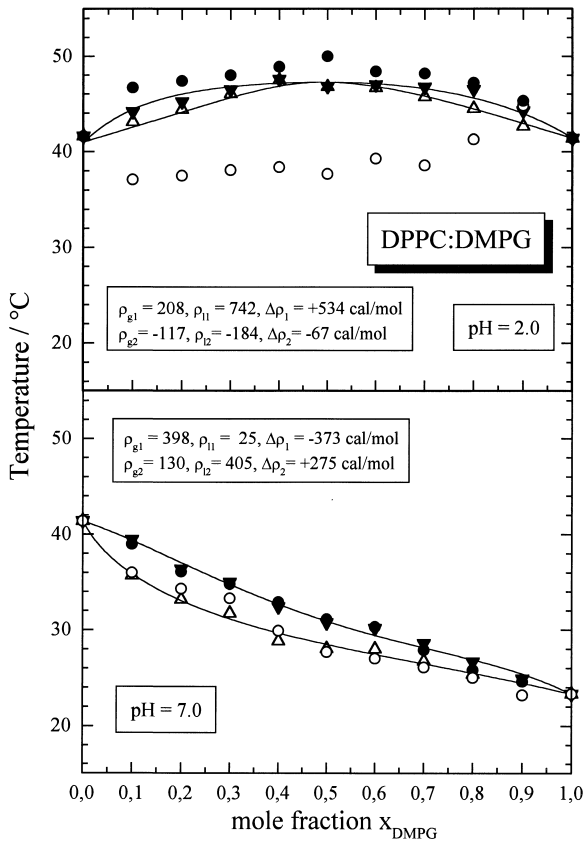

Fig. 8 Pseudobinary phase diagrams for the system DPPC/DMPG at pH 2 and pH 7 constructed from the simulated cp-curves. *Triangles* are T(–) and T(+) values obtained from the simulation of the cp-curves, *circles* are T^{exp}(–) and T^{exp}(+) values obtained by the usual empirical procedure. The *solid lines* are the coexistence lines calculated using the four-parameter model described in the text with the nonideality parameters shown in the *boxes*

DMPC/DPPG

pH 7. In this mixture a difference of two CH_2 groups is present on top of the difference in headgroup structure. Differences in chain length of the two components should lead to demixing in the gel phase of packing problems, whereas the mixing behavior in the liquid-crystalline phase should be less affected.

With increasing amount of DPPG the pretransition is first shifted to lower temperatures up to a mole fraction of 0.5 where it cannot be observed owing to experimental reasons, and then increases again. For this gel-gel transition, we therefore observe something like a phase diagram with a lower azeotropic point. However, we have not analyzed this behavior in more detail and the phase diagram in Fig. 7 does not include the pretransition behavior.

The simulation (see Fig. 3) leads to a diagram with a lower azeotropic point at $x_{DPPG} = 0.15$ or even a miscibility gap. The nonideality parameters are all negative, indicating complex formation.

pH 2. Protonation of DPPG leads to an S-shaped phase diagram with large negative nonideality parameters. For a 1 : 1 mixture, complex formation is more likely in the liquid-crystalline phase than in the gel phase, again showing that the effect of chain length difference, which partly compensates the tendency for complex formation, is more pronounced for the gel than for the liquid-crystalline phase.

DPPC/DMPG

pH 7. In the previous case the PG component had the longer chain, this is opposite for the DPPC/DMPG mixtures.

The peaks for the main phase transition are sharper compared to the system DMPC/DPPG indicating a narrower coexistence range and more ideal mixing. This is also evident from the shape of the phase diagram (Fig. 8). The DPPC/DMPG system has only positive ρ values with $\rho_{g1} > \rho_{11}$ ($\Delta\rho_1 = -373$ cal/mol). The asymmetry is positive for both phases.

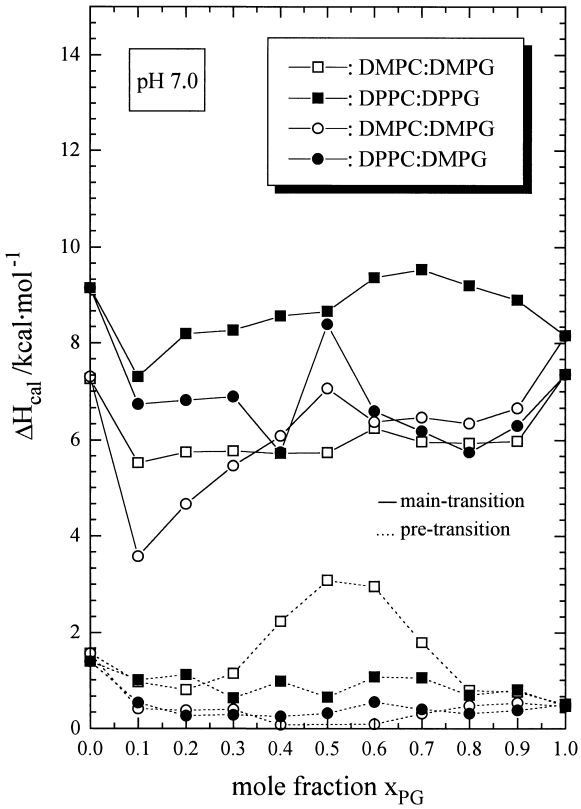

Fig. 9 Calorimetrically measured phase transition enthalpies for the main phase transition and the pretransition for various PC/PG-mixtures at pH 7

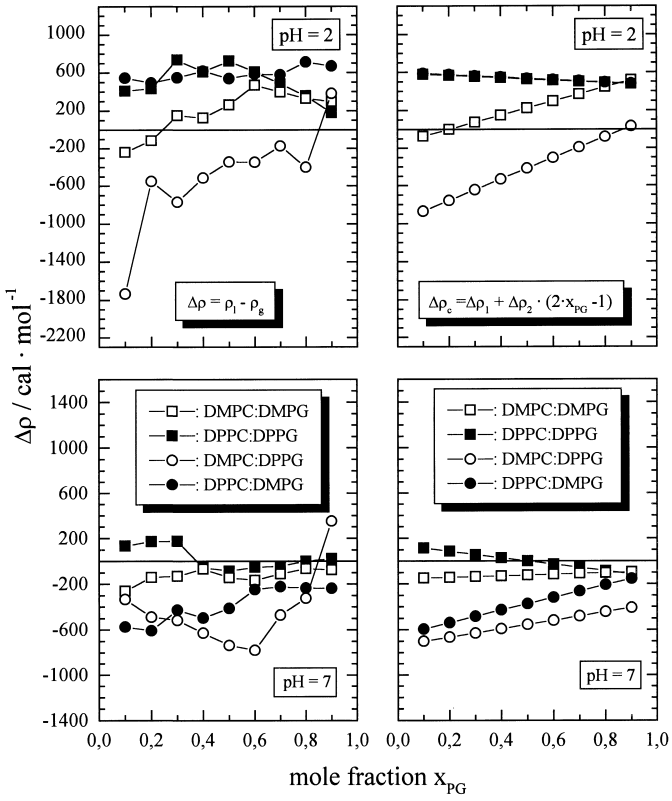

Fig. 10 *Left:* Difference in nonideality parameters $\Delta\rho = \rho_1 - \rho_g$ for PC/PG-mixtures at pH 2 and pH 7 obtained from the simulation of the cp-curves. *Right:* $\Delta\rho$-values as a function of composition calculated from the nonideality parameters shown in Figs. 5–8

pH 2. The analysis of the phase diagram suggests a system with an upper azeotropic point (see Fig. 8). The ρ_1-values for the gel and the liquid-crystalline phase are positive and very similar to those of the DPPC/DPPG system. However, the ρ_2-values are both negative and thus have opposite sign as found for DPPC/DPPG.

Discussion

Differential scanning calorimetry is one of the most efficient methods to study the mixing behavior of pseudobinary phospholipid mixtures. The established method to determine the temperatures of onset and end of melting from the experimental thermograms was improved by simulating the experimental heat capacity curves (cp^{exp}) with a model accounting for nonideal mixing in the gel ($P_{\beta'}$) as well as the liquid-crystalline (L_α) phase and taking into account the broadening of the transition due to limited cooperativity (Johann et al. 1996). The simulation of the cp^{exp}-curves give satisfactory fits for all systems at both pH values (see Figs. 1–4). From the simulation of the heat capacity curves, the temperatures T(–) and T(+) for onset and end of melting were obtained (triangles in Figs. 5–8). Also added in these figures are the corresponding temperatures $T^{exp}(-)$ and $T^{exp}(+)$ which were obtained by the established empirical procedures (Xu et al. 1987; Ali et al. 1989; Mabrey and Sturtevant 1976; Silvius and Gagné 1984 a, b). The accuracy of onset and end temperatures determined by the empirical procedure is ±1–2 °C for broad transitions because of the problem of defining the temperatures at which the DSC curves deviate from the baseline. The direct simulation is more "objective" because the influence of the experimentalist is reduced. The accuracy of the onset and end temperatures is therefore better with approximately ±0.5 °C.

The temperatures T(–) and T(+) obtained by the simulation of the heat capacity curves generally indicate narrower two-phase regions than those generated by the usual empirical methods, because the broadening by reduced cooperativity is removed. The simulations yield the nonideality parameters and the cooperative unit size as a function of composition of the mixture. This information cannot be obtained with any other method. To verify the results of the simulations of the heat capacity curves we simulated the phase diagrams with a four parameter model, which takes the nonsymmetric mixing behavior into account (Johann et al. 1996; Garidel et al. 1997).

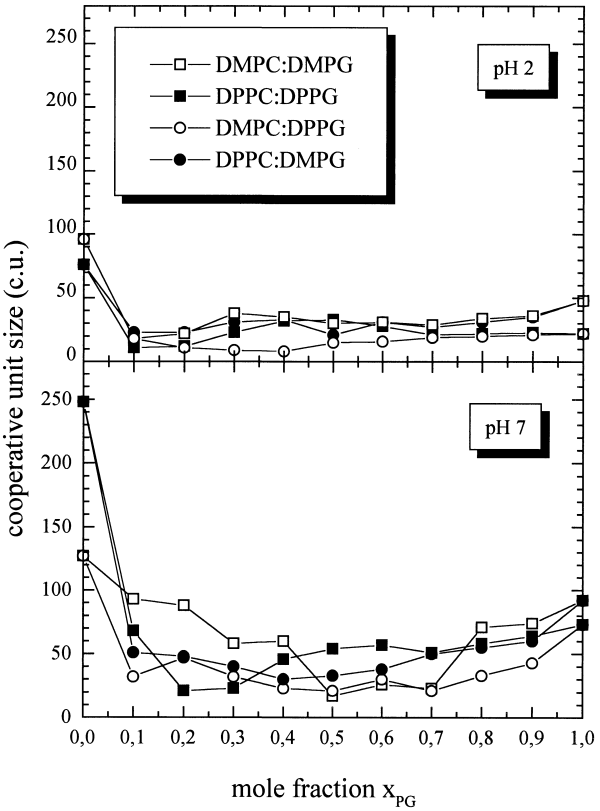

Fig. 11 Cooperative unit size c. u. for PC/PG-systems at pH 2 and pH 7

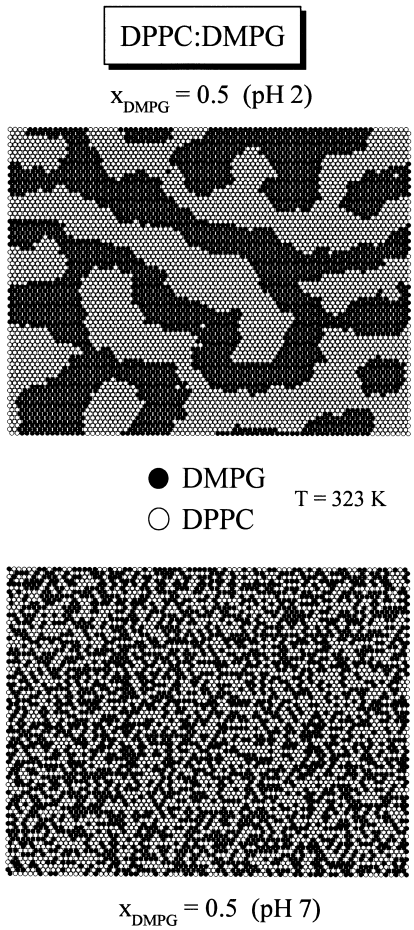

Fig. 12 Monte Carlo simulations for the system DPPC/DMPG for the lateral lipid distributions in the liquid-crystalline phase (T = 323 K) at pH 2 and pH 7. Simulation parameters: $x_{DMPG} = 0.5$; $\rho_1 = +742$ cal/mol (pH 2), $\rho_1 = +25$ cal/mol (pH 7)

Cooperative unit size c. u.

From Fig. 11 we see that PCs have higher c. u.-values than the corresponding PGs. At pH 2, all values are considerably reduced compared to the c. u. at neutral pH. The c. u.-values for mixtures are lower than those of pure components. Comparison of the c. u.-values of PC/PG mixtures at pH 7 with the corresponding values of PA/PC-mixtures (Garidel et al. 1997) shows that the c. u.-values of the PC/PG-mixtures are in the range of 30 – 40 and therefore higher than for PC/PA mixtures. The cooperativity in PC/PG mixtures is therefore more pronounced. This can be understood by considering that the similarities in the phase behavior between PC and PG are larger than for PC and PA, respectively.

The "U"-form of the plots in Fig. 11 has been suggested before by Sugár (1987) and is corroborated by our simulations. In reality, c. u. is likely to be a function of temperature (Sugár 1987). The c. u. values reported here are averaged values for the whole temperature range of the transition, but they reflect fairly accurately the expected composition dependence.

Phase diagrams

Pseudobinary systems at pH 7: equal chain lengths

PC and PG have very similar phase behavior. Both show a pretransition from an $L_{\beta'}$- to a $P_{\beta'}$-phase before the main transition into the liquid-crystalline L_α-phase (Janiak et al. 1976, 1979). The thermodynamic parameters for the main phase are also similar (see Table 1 and Figs. 1 and 2). Even the ^{2}H-NMR order parameters S_{CD} of PCs and PGs with identical chain length have similar values (Garidel 1993), indicating that the chains of the two components have similar conformational freedom in the liquid-crystalline phase.

The similarity in gel phase behavior is also obvious. We observe a pretransition for all PC/PG mixtures at pH 7 when PG is singly charged (Figs. 1 – 4). The temperatures and the transition enthalpies of this pretransition depend on the type of system studied. An increase of ΔH_p for equimolar mixtures (see Fig. 9) is observed for the system DMPC/DMPG. A similar trend has been found before by Findlay and Barton (1978). In the other mixtures the behavior of the pretransition as a function of composition is

less clear. It is likely that some effects can be caused by different cooling protocols because T_p and also ΔH_p depend on the cooling rates and the lowest temperature achieved during cooling. We have not investigated these effects any further but have concentrated on the analysis of the main phase transition.

Mixtures of DMPC/DMPG and DPPC/DPPG (pH 7) show nearly ideal miscibility and the phase diagrams have similar shapes. The coexistence range is very narrow (ca. 0.1 °C). The empirically determined temperatures $T^{exp}(-)$ and $T^{exp}(+)$ show somewhat larger differences than the T(–) and T(+) values, but indicate essentially the same phase behavior. The nonideality parameters ρ_1 and ρ_g (Figs. 5 and 6) and also the difference $\Delta\rho$ (Fig. 10) are only slightly composition dependent.

Pseudobinary systems at pH 7: unequal chain lengths

In pseudobinary systems with unequal chain length, e. g. in the systems DMPC/DPPG and DPPC/DMPG, we observe phase diagrams with a broadened coexistence range and different mixing behavior depending on whether the PC or the PG component has the longer acyl chain. For DMPC/DPPG, the coexistence range is wider due to the larger difference in T_m-values of the pure components than for DPPC/DMPG. This indicates larger deviations from ideal mixing for the former system. This is also directly evident from the thermograms in Figs. 3 and 4. The deviation of the empirically determined onset and end of melting temperatures from those obtained from the direct simulations of the thermograms (Figs. 7 and 8) is here much larger. Therefore, nonideality parameters for DMPC/DPPG mixtures determined from the empirically determined temperatures would be completely different than those ρ-values reported here.

The phase diagram of DMPC/DPPG at pH 7 indicates a lower azeotropic point at $x_{DPPG} = 0.15$. Large negative ρ_1 values are observed for both phases and also a large negative $\Delta\rho_1$ of –554 cal/mol. Both values for ρ_2, describing the asymmetry of mixing, are negative, i. e. mixtures with high amounts of DPPG shows an increase in complex formation between unlike molecules. At low PG content the nonideality in the gel phase decreases, the ρ-values becomes almost zero, whereas for the liquid-crystalline phase the ρ-value stays negative. In the gel phase at low PG content, the tendency for complex formation is compensated by the demixing tendency of unlike chains. However, at high PG content complex formation between unlike molecules is preserved, i. e. the incorporation of the shorter chain DMPC into gel phase DPPG leads to complexes of these two molecules.

In DPPC/DMPG, DPPC has the longer chain and a different phase behavior is observed. Here, the liquid-crystalline phase behaves almost ideally, whereas the positive nonideality parameter ρ_1 for the gel phase indicates demixing (see Figs. 4 and 8). The asymmetry is positive for both phases. Mixtures with high DMPG content show greater tendency towards demixing than those with low DMPG content. A Monte Carlo simulation for the liquid-crystalline phase for $x_{DMPG} = 0.5$ at 50 °C shows a relatively homogeneous lateral distribution of both components, as expected from the low ρ_1-value of +25 cal/mol (see Fig. 12).

Pseudobinary systems at pH 2

Changing the pH to 2 decreases the headgroup charge of pure PGs and leads to an increase in transition temperature due to the decrease in electrostatic repulsion between the headgroups and the increase in capacity to form attractive intermolecular hydrogen bonds (see discussion above). Furthermore, the protonation of PGs also affects the fluidity and molecular mobility of the lipids in the bilayer plane (Watts and Marsh 1981). The fluidity is greater for charged PGs compared to their protonated state (Watts et al. 1978).

Under physiological conditions at pH 7, PCs and PGs have gel phases with tilted chains (Watts et al. 1981). In the protonated state, the tilt angle of PGs is markedly reduced. This implies that at pH 2 a PC gel phase with tilted chains has to be mixed with a PG gel phase with non-tilted chains. This will severely influence the mixing properties in the PC/PG-system in the gel phase, but in the liquid-crystalline phase this effect will be absent.

The thermograms of the four systems are considerably different compared to those measured at pH 7 (see Figs. 1–4) because the pure PG component has now a higher T_m in mixtures with equal chain lengths. In DPPC/DMPG at pH 2, however, both components have now almost the same T_m, whereas in DMPC/DPPG the difference in phase transition temperatures is enhanced by the change in pH to 2.

Equal chain lengths

The two mixtures behave differently (see thermograms in Figs. 1 and 2 and phase diagrams in Figs. 5 and 6). For DMPC/DMPG, the nonideality parameters are negative for both phases. The tendency for complex formation in the gel phase is somewhat larger than in the liquid-crystalline phase. The asymmetry in mixing behavior is large and negative. Adding DMPG to DMPC leads to complex formation of unlike molecules. The shape of the phase diagram seems to indicate an upper azeotropic point at $x_{DMPG} = 0.7 - 0.9$ or even a miscibility gap in this region. The plot of $\Delta G_{mix} = \Delta G^{ideal} + \Delta G^{E}$ as a function of mole fraction using the nonideality parameters requires that $(\partial^2 \Delta G_{mix}/\partial x^2)_{p,T} > 0$ over the whole range of compositions, if the components are still miscible. The calculation shows that this is still the case (data not shown). Therefore, azeotropic behavior is more likely.

For DPPC/DPPG mixtures with positive nonideality parameters are found for both phases. The phase diagram (Fig. 6) shows a relatively flat liquidus curve over a larger mole fraction range. Again, a plot of $(\partial^2 \Delta G_{mix}/\partial x^2)_{p,T}$ using the nonideality parameters from the simulations is

still positive over the whole concentration range, an upper azeotropic point is likely.

Unequal chain lengths

For DMPC/DPPG at pH 2, the difference in T_m-values for the pure components has increased to 33 °C. We find an S-shaped phase diagram and negative nonideality parameters for both phases, indicating complex formation between unlike molecules. This diagram resembles the phase diagram of the DMPC/DMPG mixture at pH 2.

When the chain length of the two compounds is reversed (DPPC/DMPG), the phase diagram indicates an upper azeotropic point (Fig. 8). This phase diagram is similar to that of DPPC/DPPG at pH 2. It seems as if the mixing behavior is always determined by the PC component in the mixture, because the two mixtures containing either DMPC or DPPC behave similarly.

A high and positive ρ-value is an indication of clustering of like molecules in the liquid-crystalline phase (Wu and McConnell 1975; Luna and McConnell 1977; von Dreele 1978; Hinderliter et al. 1994; Garidel et al. 1997). This is illustrated by a Monte Carlo simulation (Kawasaki 1972; Jan et al. 1984; Garidel et al. 1997) of the equimolar DPPC/DMPG mixture at pH 2, which shows the lateral distribution of both components in the mixture (see Fig. 12). The figure shows large domains of like molecules in the fluid phase.

Comparison with PC/PA mixtures

We have studied before the miscibility of PC/PA systems of different chain length and at different pH values (Garidel et al. 1997). PA is also negatively charged at pH 7 and at pH 4 it is partly protonated. However, the behavior of PC/PG mixtures is considerably different from that of PC/PA. This is not completely surprising, because pure electrostatic effects are thought to play only a minor role. Far more important are headgroup interactions with neighboring lipid and with water molecules. Both PC/PA mixtures with equal chain lengths show highly negative nonideality parameters ρ_1 at pH 7, whereas for the DPPG/DPPC mixture almost ideal miscibility is observed in the liquid-crystalline as well as the gel phase and the DMPC/DMPG mixture shows a slight tendency towards the formation of complexes. At pH 4, the PC/PA mixtures display a tendency to demix in the liquid-crystalline phase but to form complexes in the gel phase. In the corresponding PC/PG mixtures the behavior depends on the chain length. For shorter chain PCs, both ρ-values are negative, but for the mixture with the longer chain PCs, they are positive.

Some analogies are observed for systems with unequal chain length. For DPPC/DMPA we observe a miscibility gap at pH 4. In the corresponding DPPC/DMPG system at pH 2 the system is also close to demixing, we observe an upper azeotropic point. This similarity is not observed, when the chain lengths are reversed. For DMPC/DPPA at pH 4 positive ρ-value for the liquid-crystalline phase (demixing) is found and the ρ-value for the gel phase remains negative (complex formation). However, in the corresponding DMPC/DPPG mixtures at pH 2, both ρ-values are negative, indicating complex formation of unlike molecules in both phases.

Summary and conclusion

The phase behavior of PC/PG mixtures was studied as a function of pH and chain length using a newly developed simulation method for a direct determination of the temperatures for the onset and end of the phase transition and the nonideality parameters from the DSC curves. Compared with older empirical methods our procedure is a new and better way to construct and analyze phase diagrams (Johann et al. 1996; Garidel et al. 1997).

The miscibility in PC/PG mixtures depends on the charge of the PG component. At pH 7, PGs are negatively charged and the PC headgroups are zwitterionic. With the exception of DMPC/DPPG, all mixtures show relatively low nonideality parameters which can be slightly negative or positive, indicating nearly ideal miscibility. For DMPC/DPPG the phase diagram seems to indicate a lower azeotropic point, the nonideality parameters are negative.

At pH 2, the PG headgroup is mainly protonated (>90%, Tuchtenhagen, 1994), while the PC headgroup is still mainly zwitterionic. In the gel phase, the tilt angle of protonated PG is significantly reduced. The mixing behavior changes drastically. When the PC component has the short chain, i. e. DMPC, we observe phase diagrams with negative nonideality parameters indicating complex formation between like molecules. For mixtures with DPPC as the PC component we see phase diagrams with upper azeotropic points and positive nonideality parameters. Protonation of DPPG leads to clustering of like molecules in the liquid-crystalline phase.

It is obvious that the mixing behavior is a complicated function of headgroup and chain length properties. The subtle differences between attractive interactions between headgroups via hydrogen bonds and repulsive electrostatic interactions in combination with chain length differences between the two compounds can lead to unexpected mixing behavior as a function of the absolute chain length and the chain length differences between the two lipid components.

Acknowledgements We thank M. Agostinho and B. Göbelt for their technical help. This work was supported by the Deutsche Forschungsgemeinschaft (Bl 182/7-3) and the Fonds der Chemischen Industrie.

References

Ali S, Lin H-N, Bitman R, Huang C-H (1989) Binary mixtures of saturated and unsaturated mixed-chain phosphatidylcholines. A differential scanning calorimetry study. Biochemistry 28: 522–528

Almeida PFF, Vaz WLC, Thompson TE (1993) Percolation and fusion in three-component bilayers: effect of cholesterol on an equimolar mixture of two phosphatidylcholines. Biophys J 64: 399–412

Almeida PPF, Vaz WLC (1995) Lateral diffusion in membranes. In: Lipowsky R, Sackmann E (eds) Structure and dynamics of membranes. Elsevier, Amsterdam, pp 305–357

Bangham AD, Morley CJ, Phillipips MC (1979) The physical properties of an effective lung surfactant. Biochim Biophys Acta 573: 552–556

Barton PG, Findlay EJ (1978) A lipid phase separation model for prothrombin activation. DHEW Publ (US) NIH 78-1087, 461–470

Benson BJ, Williams MC, Hawgood S, Sargeant T (1984) Role of lung surfactant-specific proteins in surfactant structure and function. Prog Resp Res 18: 83–92

Blume A (1988) Applications of calorimetry to lipid model membranes. In: Hidalgo C (ed) Physical properties of biological membranes and their functional implications. Plenum Press, New York pp 71–121

Blume A (1991) Biological calorimetry: membranes. Thermochim Acta 193: 299–347

Blume A, Eibl H (1979) The influence of charge on bilayer membranes. Calorimetric investigations of phosphatidic acid bilayers. Biochim Biophys Acta 558: 13–21

Bogg JM (1987) Lipid intermolecular hydrogen bonding: influence on structural organization and membrane function. Biochim Biophys Acta 906: 353–404

Borle F, Seelig J (1985) Ca^{2+} binding to phosphatidylglycerol bilayers as studied by differential scanning calorimetry and ^{2}H- and ^{31}P-nuclear magnetic resonance. Chem Phys Lipids 36: 263–283

Brumbaugh EE, Huang C (1992) Parameter estimation in binary mixtures of phospholipids. Methods Enzym 210: 521–539

Cevc G, Watts A, Marsh D (1980) Non-electrostatic contribution to the titration of the ordered – fluid phase transition of phosphatidylglycerol bilayers. FEBS Lett 120: 267–270

Clements JA (1977) Function of the alveolar lining. Am Rev Respir Dis 115: 67–71

Creuwels LAJM, van Golde LMG, Haagsman HP (1996) Surfactant protein B: effects on lipid domain formation and intermembrane lipid flow. Biochim Biophys Acta 1285: 1–8

Cronan JE, Gelman EP (1975) Physical properties of membrane lipids: biological relevance and regulation. Bact Rev 39: 232–256

Dombrose FA, Gitel SN, Zawalich K, Jackson CM (1979) The association of bovine prothrombin fragment 1 with phospholipid. J Biol Chem 254: 5027–5040

Eibl H, Woolley P (1979) Electrostatic interactions at charged lipid membranes. Hydrogen bonds in lipid membrane surface. Biophys Chem 10: 261–271

Eklund KK, Salonen IS, Kinnunen PJ (1989) Monovalent cation dependent phase behavior of dipalmitoylphosphatidylglycerol. Chem Phys Lipids 50: 71–78

Findlay EJ, Barton PG (1978) Phase behavior of synthetic phosphatidylglycerols and binary mixtures with phosphatidylcholines in the presence and absence of calcium ions. Biochemistry 17: 2400–2405

Garidel P (1993) Physikalisch-chemische Untersuchungen zum thermotropen Verhalten von Phospholipiden. Anwendungen der DSD-, DSC-, ^{2}H-NMR- und FT-IR-Methoden. Diploma thesis, University of Kaiserslautern, Germany

Garidel P, Johann C, Blume A (1997) Nonideal mixing and phase separation in phosphatidylcholine-phosphatidic acid mixtures as a function of acyl chain length and pH. Biophys J 72: 2196–2210

Glaser M (1993) Lipid domains in biological membranes. Curr Opin Struct Biol 3: 475–481

Goerke J (1974) Lung surfactant. Biochim Biophys Acta 344: 241–261

van Golde LMG, Batenburg JJ, Robertson B (1988) The pulmonary surfactant system: Biochemical aspects and functional significance. Physiol Rev 8: 374–455

Hahn FL, Luckhaus R (19569 Ein vorzügliches Reagenz zur kolorimetrischen Bestimmung von Phosphat und Arsenat. Z Anal Chem 149: 172–177

Harlos K, Eibl H (1980) Influence of calcium on phosphatidylglycerol. Two separate lammellar structures. Biochemistry 19: 895–899

Hinderliter AK, Huang J, Feigenson GW (1994) Detection of phase separation in fluid phosphatidylserine/phosphatidylcholine mixtures. Biophys J 67: 1906–1911

Hoekstra D (1982 a) Fluorescence method for measuring the kinetics of Ca^{2+} induced phase separations in phosphatidylserine-containing lipid vesicles. Biochemistry 21: 1055–1061

Hoekstra D (1982 b) Role of lipid phase separations and membrane hydration in phospholipid vesicle fusion. Biochemistry 21: 2833–2840

Jackson CM, Owen W, Gitel SN, Esmon CT (1974) The chemical role of lipids in prothrombin conversion. Thromb Haemostasis 17: 273–293

Jacobson K, Papahadjopoulos D (1975) Phase transitions and separations in phospholipid membranes induced by changes in temperature, pH, and concentration of bivalent cations. Biochemistry 14: 152–161

Jan H, Lookman T, Pink DA (1984) On computer simulation methods used to study models of two-component lipid bilayers. Biochemistry 23: 3227–3231

Janiak MJ, Small DM, Shipley GG (1976) Nature of the thermal pretransition of synthetic phospholipids: dimyristoyl- and dipalmitoyllecithin. Biochemistry 15: 4575–4580

Janiak MJ, Small DM, Shipley GG (1979) Temperature and compositional dependence of the structure of hydrated dimyristoyllecithin. J Biol Chem 254: 6068–6078

Johann C, Garidel P, Mennicke L, Blume A (1996) New approaches to the simulation of heat-capacity curves and phase diagrams of pseudobinary phospholipid mixtures. Biophys J 71: 3215– 3228

Kawasaki K (1972) Kinetics of Ising models. In: Domb C, Green MS (eds) Phase transitions and critical phenomena. Academic Press, London, pp 443–501

Lau A, McLaughlin A, McLaughlin S (1981) The adsorption of divalent cations to phosphatidylglycerol bilayer membranes. Biochim Biophys Acta 645: 279–292

Lee AG (1975 a) Functional properties of biological membranes: a physical-chemical approach. Prog Biophys Mol Biol 29: 3–56

Lee AG (1975 b) Fluorescence studies of chlorophyll incorporated into lipid mixtures, and the interpretation of "phase" diagrams. Biochim Biophys Acta 413: 11–23

Lee AG (1977 a) Lipid phase transitions and phase diagrams. I. Lipid phase transitions. Biochim Biophys Acta 472: 237–281

Lee AG (1977 b) Lipid phase transitions and phase diagrams. II. Mixtures involving lipids. Biochim Biophys Acta 472: 285–344

Lee AG (1978) Calculation of phase diagrams for non-ideal mixtures of lipids, and a possible random distribution of lipids in lipid mixtures in the liquid crystalline phase. Biochim Biophys Acta 507: 433–444

Lee AG, Birdsall NJM, Metcalfe JC, Toon PA, Warren GP (1974) Clusters in lipid bilayers and the interpretation of thermal effects in biological membranes. Biochemistry 13: 3699–3705

Lentz BL, Alford DR, Hoechli M, Dombrose FA (1982) Phase behavior of mixed phosphatidylglycerol/phosphatidylcholine multilamellar and unilamellar vesicles. Biochemistry 21: 4212–4219

Luna EJ, McConnell HM (1977) Lateral phase separations in binary mixtures of phospholipids having different charges and different crystalline structures. Biochim Biophys Acta 470: 303–316

Mabrey S, Sturtevant JM (1976) Investigation of phase transition of lipids and lipid mixtures by high sensitivity differential scanning calorimetry. Proc Natl Acad Sci USA 73: 3862–3866

MacDonald PM, Seelig J (1987) Calcium binding to mixed phosphatidylglycerol-phosphatidylcholine bilayers as studied by deuterium magnetic resonance. Biochemistry 26: 6292–6298

MacFarlane MG (1964) Phosphatidylglycerols and lipoamino acids. Adv Lipid Res 2: 91–125

Mennicke L (1995) Die Simulation der Wärmekapazitätskurven und die Berechnung der Phasendiagramme von pseudobinären Lipid-Lipid-Wasser-Systemen am Beispiel von gemischtkettigen Phospholipiden mit verzweigten Acylketten. PhD thesis, University of Kaiserslautern, Germany

Metcalf TN, Wang JL, Schindler M (1986) Lateral diffusion of phospholipids in the plasma membrane of soybean protoplasts: Evidence for membrane lipid domains. Proc Natl Acad Sci USA 83: 95 – 99

Ranck JL, Keira T, Luzzati V (1977) A novel packing of the hydrocarbon chains in lipids. The low temperature phases of dipalmitoylphosphatidylglycerol. Biochim Biophys Acta 488: 432 – 441

Sacré MM, Hoffmann W, Turner M, Tocanne J-F, Chapman D (1979) Differential scanning calorimetry studies of some phosphatidylglycerol lipid-water systems. Chem Phys Lipids 69: 69 – 83

Seelig J, Lehrmann R, Terzi E (1995) Domain formation induced by lipid-ion and lipid-peptide interactions. Mol Membrane Biol 12: 51 – 57

Shimshick EJ, McConnell HM (1973) Lateral phase separation in phospholipid membranes. Biochemistry 12: 2351 – 2360

Silvius JR, Gagné J (1984 a) Lipid phase behavior and calcium induced fusion of phosphatidylethanolamine-phosphatidylserine vesicles. Calorimetric and fusion studies. Biochemistry 23: 3232 – 3240

Silvius JR, Gagné J (1984 b) Calcium-induced fusion and lateral phase separation in phosphatidylcholine-phosphatidylserine vesicles. Correlation by calorimetric and fusion measurements. Biochemistry 23: 3241 – 3247

Stier A, Sackmann E (1973) Spin labels as enzyme substrates. Heterogeneous lipid distribution in liver microsomal membranes. Biochim Biophys Acta 311: 400 – 408

Sugàr IP (1987) Cooperativity and classification of phase transitions. Application to one- and two-component phospholipid membranes. J Phys Chem 91: 95 – 101

Suzuki U, Fujita Y, Kogishi K (1989) Reconstitution of tubular myelin from synthetic lipids and proteins associated with pig pulmonary surfactant. Am Rev Resp Dis 115: 75 – 81

Tenchov B (1985) Nonuniform lipid distribution in membranes. Prog Surf Sci 20: 273 – 340

Tocanne J-F, Cézanne L, Lopez A, Piknova B, Schram V, Tournier J-F, Welby M (1994) Lipid domains and lipid/protein interactions in biological membranes. Chem Phys Lipids 73: 139 – 158

Tocanne J-F, Teissié J (1990) Ionization of phospholipids and phospholipid-supported interfacial lateral diffusion of protons in membrane model systems. Biochim Biophys Acta 1031: 111 – 142

Träuble H (1976) Membrane electrostatics. In: Abrahamsson S, Pascher I (eds) Structure of biological membranes. Plenum Press, New York, pp 509 – 550

Träuble H, Eibl H (1974) Electrostatic effects on lipid phase transitions: membrane structure and ionic environment. Proc Natl Acad Sci USA 71: 214 – 221

Träuble H, Teubner M, Woolley P, Eibl H (1976) Electrostatic interactions at charged lipid membranes. 1. Effects of pH and univalent cations on membrane structure. Biophys Chem 4: 319 – 342

Tuchtenhagen J (1994) Kalorimetrische und FT-IR-spektroskopische Untersuchungen an Phospholipidmodellmembranen. PhD thesis, University of Kaiserslautern, Germany

van Dijck PWM, Ververgaert PHJTh, Verkleij AJ, van Deenen LLM, De Gier J (1975) Influence of Ca^{2+} and Mg^{2+} on the thermotropic behavior and permeability properties of liposomes prepared from dimyristoyl phosphatidylglycerol and mixtures of dimyristoyl phosphatidylglycerol and dimyristoyl phosphatidylcholine. Biochim Biophys Acta 406: 465 – 478

van Dijck PWM, Kaper AJ, Oonk HAJ, De Gier J (1977) Miscibility properties of binary phosphatidylcholine mixtures. A calorimetric study. Biochim Biophys Acta 470: 58 – 69

van Dijck PWM, de Kruiff B, Verkeij AJ, van Deenen LLM, De Gier J (1978) Comparative studies on the effects of pH and Ca^{2+} on bilayers of various negatively charged phospholipids and their mixtures with phosphatidylcholine. Biochim Biophys Acta 512: 84 – 96

Vaz WLC (1994) Diffusion and reaction in phase-separated membranes. Biophys Chem 50: 139 – 145

Vaz WLC (1995) Percolation properties of two-component, two-phase phospholipid bilayers. Mol Membrane Biol 12: 39 – 43

Verkleij AJ, De Kruyff B, Ververgaert PH, Tocanne JF, van Deenen LLM (1974) The influence of pH, Ca^{2+} and protein on the thermotropic behavior of the negatively charged phospholipid, phosphatidylglycerol. Biochim Biophys Acta 39: 432 – 437

van Dreele PH (1978) Estimation of lateral species separation from phase transitions in non-ideal two-dimensional lipid mixtures. Biochemistry 17: 3939 – 3943

Watts A, Harlos K, Marsh D (1981) Charged induced tilt in ordered phase phosphatidylglycerol bilayers. Evidence from x-ray diffraction. Biochim Biophys Acta 645: 91 – 96

Watts A, Harlos K, Maschke W, Marsh D (1978) Control of the structure and fluidity of phosphatidylglycerol bilayers by pH titration. Biochim Biophys Acta 510: 63 – 74

Watts A, Marsh D (1981) Saturation transfer ESR studies of molecular motion in phosphatidylglycerol bilayers in the gel phase. Effects of pretransitions and pH titration. Biochim Biophys Acta 642: 231 – 241

Wiedmann T, Salmon A, Wong V (1993) Phase behavior of mixtures of DPPC and POPG. Biochim Biophys Acta 1167: 114 – 120

Wohlgemuth R, Waespe-Sarvcevic N, Seelig J (1980) Bilayers of phosphatidylglycerol. A deuterium and phosphorus nuclear magnetic resonance study of the head-group-region. Biochemistry 19: 3315 – 3321

Wu SH, McConnell HM (1975) Phase separation in phospholipid membranes. Biochemistry 14: 847 – 854